Original Article
https://doi.org/10.5115/acb.2017.50.3.187
pISSN 2093-3665 eISSN 2093-3673
Anatomy & Cell Biology acb

Histological study on the effect of nicotine on adult male guinea pig thin skin

Sohair A. Eltony, Safaa S. Ali
Department of Histology and Cell Biology, Faculty of Medicine, Assiut University, Assiut, Egypt

Abstract: Tobacco smoking has been identified as an important factor in premature skin aging to detect the histological changes occurred in adult male guinea pig thin skin under the influence of low and high doses of nicotine; which constitutes approximately 0.6%–3.0% of the dry weight of tobacco. Fifteen adult male pigmented guinea pigs were equally divided into three groups: group I, control; group IIA, low dose nicotine treated; 3 mg/kg subcutaneously for 4 weeks; and group IIB, high dose nicotine treated; 6 mg/kg subcutaneously for 4 weeks. Specimens from the back thin skin were processed for light and electron microscopy. Nicotine administration revealed flattened dermo-epidermal junction and reduced rete ridges formation. Collagen bundles were disorganized with increased spaces between them. A reduction in the amount of elastic fibers in the dermis were also observed compared to group I. Ultrastructurally, keratinocytes had hyperchromatic nuclei, intracytoplasmic vacuoles, disruption of desmosomal junctions, irregular tonofilaments distribution, and increased inter-cellular spaces. These changes were more pronounced with high dose nicotine administration. The epidermal thickness was reduced in low dose nicotine administration. But, high dose nicotine administration revealed increased epidermal thickness compared to the control group. Nicotine induced structural changes of adult male guinea pig thin skin. These changes were more pronounced with high dose nicotine administration.

Key words: Nicotine, Thin skin, Guinea pigs

Received March 22, 2017; Revised April 14, 2017; Accepted May 16, 2017

Introduction

The prevalence of tobacco smoking appears to be increasing in the World Health Organization Eastern Mediterranean Region and the African Region. In 2015, over 1.1 billion people, far more males than females, smoked tobacco. Nicotine is an alkaloid derived from the tobacco plant "Nicotiana tabacum." It constitutes approximately 0.6%–3.0% of the dry weight of tobacco and is present in the range of 2–7 μg/kg of various edible plants [1]. The role of nicotine in mammals is more controversial. In lesser doses (an average cigarette yields about 1 mg of absorbed nicotine), the substance acts as a stimulant [2]. This stimulant effect is likely to be a major contributing factor to the dependence-forming properties of tobacco smoking [3]. On the contrary, high amounts (50–100 mg) can be harmful [4].

The skin is one of the largest organs in the body in surface area and weight. It acts as a barrier; from mechanical impacts and pressure, variations in temperature, microorganisms, radiation, and chemicals. It also regulates body temperature via sweat and hair, and changes in peripheral circulation and fluid balance via sweat. It also acts as a reservoir for the synthesis of vitamin D. The skin is an organ of sensation as it contains an extensive network of nerve cells that detect and relay changes in the environment [5].

Nicotinic receptors are expressed in the skin; on keratinocytes, fibroblasts, and blood vessels [4]. Based on epide-

Corresponding author:
Sohair A. Eltony
Department of Histology and Cell Biology, Faculty of Medicine, Assiut University, Assiut 71111, Egypt
Tel: +20-01001031153, Fax: +20-0882080278, E-mail: sohair_eltony@yahoo.com

miological studies tobacco smoking has been identified as an important factor in premature skin aging [6-8]. The improvement of skin quality has gained particular attention as skin mirrors natural aging [9, 10].

Therefore, this study aimed to detect the histological changes occurred in adult guinea pig thin skin under the influence of low and high doses of nicotine.

Material and Methods

A total number of 15 adult (4 months old) male pigmented "discolors" guinea pigs (450–600 g body weight) were used in this study. They were purchased from Central Animal House, Faculty of Medicine, Assiut University. All animal procedures were in accordance with the standards set forth in guidelines for the care and use of experimental animals by Committee for Purpose of Supervision of Experiments on Animals (CPCSEA) and according to National Institute of Health (NIH) protocol, and approved by the Institutional Ethics Committee of Assiut University. The animals were housed in clean capacious cages under standard conditions (light, temperature with food, and water provided ad libitum).

Animal groups

The animals were divided into two main groups.

- Group I (control): consisted of five guinea pigs that were subcutaneously injected with 0.5 ml sterile saline 0.9% daily for 4 weeks.

- Group II (nicotine treated): consisted of 10 guinea pigs that were subcutaneously injected with nicotine hydrogen tartrate salt (1-methyl-2-(3-pyridyl) pyrrolidine-bitartrate salt; Sigma, St. Louis, MO, USA). Nicotine dose was dissolved in 0.5 ml sterile saline 0.9%. This group was equally subdivided into two subgroups, according to the dose of nicotine; five animals each: subgroup IIA (low dose nicotine treated), injected subcutaneously with nicotine at a dose of 3 mg/kg daily for 4 weeks; subgroup IIB (high dose nicotine treated), injected subcutaneously with nicotine at a dose of 6 mg/kg daily for 4 weeks. The nicotine doses (3 mg/kg and 6 mg/kg) were chosen to approximate the plasma levels reported in moderate and heavy smokers, respectively [11, 12].

This study used discolors (white and brown) male guinea pigs so that epidermal sampling could be controlled. Males were selected to exclude oestrogenic influences.

At the end of the experiment, the animals were anesthetized with ether and an area (2×3 cm) on the back thin skin was shaved and 1 cm specimens of full thickness brown skin were dissected out immediately. The specimens from each animal were cut and immersed in the appropriate fixative for light and electron microscopic examination.

Light microscopy

Full thickness skin specimens (5 mm) were immersed into 10% neutral buffered formalin for 48 hours. Then, the specimens were processed for the preparation of paraffin blocks. Paraffin sections (5 μm) were cut serially using a microtome (Leica RM 2125RT, Wetzlar, Germany), mounted on glass slides, and every 10th section was stained with hematoxylin and eosin (H&E) stain. In addition, selected sections were processed for Masson's trichrome stain for demonstration of collagen fibers and Orcein stain for demonstration of elastic fibers [13].

Electron microscopy

Skin specimens were cut into thin slices (1×1 mm) and immersed in 4% glutaraldehyde in cacodylate buffer (pH 7.4) for 24 hours and post fixed in 1% osmium tetroxide in phosphate buffer for 2 hours. Tissues were rinsed in the same buffer, dehydrated with alcohol, cleared with propylene oxide and embedded in Epon-812 substitute (cat. No. 02635, SPI-Pon Araldit Kit, AB., SPI Supplies, West Chester, PA, USA). For Polymerization, the embedded samples were kept in the incubator at 35°C, 45°C, and 60°C for 1 day each [14]. Semi-thin sections (0.5–1 μm) were cut with glass knives on the ultramicrotome (LKB Bromma 8800 Ultratome III, 3518, Stockholm-Bromma, Sweden) and stained with 1% toluidine blue (pH 7.3) for examination on a light microscope (Bx50, Model Bx50F-3, SC09160, Olympus, Tokyo, Japan). Ultrathin sections (50–80 nm) were cut from selected areas of the blocks on a Reichert ultramicrotome (Leica WILDM3Z, 89386, Wien, Austria) placed on copper grids (G 300, 3.05 mm, Polaron Equipment Ltd., Watford, UK) and contrasted with uranyl acetate and lead citrate. These sections were examined using the transmission electron microscope (Jeol E.M.-100 CX11, Japanese Electron Optic Laboratory, Tokyo, Japan) and photographed at 80 kV.

Using computer-assisted image analysis (AnalySIS-2004, Soft Imaging System, Olympus), the thickness of the epidermis in micrometers was measured by the arbitary distance method, measurement was done viewing H&E-stained sections using a 10× objective lens in five non-overlapping fields in 10 randomly chosen sections/animal. On measuring the

thickness, three measurements were taken along the length of the epidermis/field and the mean value of these measures was taken; the first measure was at medial end of the epidermis, the second was at its lateral end and the third was at the middle [15]. The rete ridges length in micrometers was measured by the arbitrary distance method, measurement was done viewing H&E-stained sections using a 40× objective lens in five non-overlapping fields in 10 randomly chosen sections/animal. The number of melanocytes per mm^2 was counted by touch count method viewing H&E-stained sections using ×100 oil immersion lens in five non-overlapping fields in 10 randomly chosen sections from three different animals for each group.

Statistical analysis

The morphometric data of each animal group were statistically analyzed using the computer statistics Prism-5.0 package (GraphPad Software Inc., San Diego, CA, USA). One-way analysis of variance (ANOVA) followed by Newman-Keuls test as a post-test was employed to compare the studied animal group. *P*-value of <0.05 was considered significant.

Results

Light microscopy

Epidermis

Group I (control) revealed the normal histological structure of the guinea pig thin skin (Fig. 1A); which resembled that of the human. The epidermis was formed of a keratinized stratified squamous epithelium resting on an irregular basement membrane at the dermo-epidermal junction (DEJ) forming well developed rete ridges. The thickness of the epidermis ranged from 61.0 to 193.8 μm (mean, 106.4±24.5 μm) (Table 1, Fig. 2). The rete ridges length ranged from 232.0 to 1,101 μm (mean, 548.4±334.8 μm) (Table 2, Fig. 3). The majority of the epidermal cells were the keratinocytes that arranged into four layers. Keratinocytes in the stratum basale were low columnar with oval nuclei. Melanocytes contained cytoplasmic brown melanin pigment, were observed in the basal layer. Their number ranged from 3 to 6 per mm^2 (mean, 4.5±1.2) (Table 3, Fig. 4). Keratinocytes in the stratum spinosum were polyhedral with central rounded nuclei. The stratum granulosum consisted of spindle shaped keratinocytes, aligned parallel to the skin surface and filled with intracytoplasmic basophilic keratohyalin granules. The stratum corneum formed of acidophilic scales. Nicotine treated groups (IIA and IIB) revealed flattened DEJ and reduced rete ridges formation (Fig. 1B, C). The thickness of the epidermis in group IIA was significantly decreased compared to group I. It ranged from 39.2 to 105.9 μm (mean, 67.2±15.5 μm) (Table 1, Fig. 2). On the contrary, the thickness of the epidermis in

Table 1. Mean epidermal thickness (μm) in the studied groups

	Group I	Group IIA	Group IIB	*P*-value
Mean±SD	106.4±24.5	67.2±15.5	109.9±73.8	0.001[a]
Range	61.0–193.8	39.2–105.9	41.3–461.2	

[a]Group I vs. Group IIB (*P*>0.05).

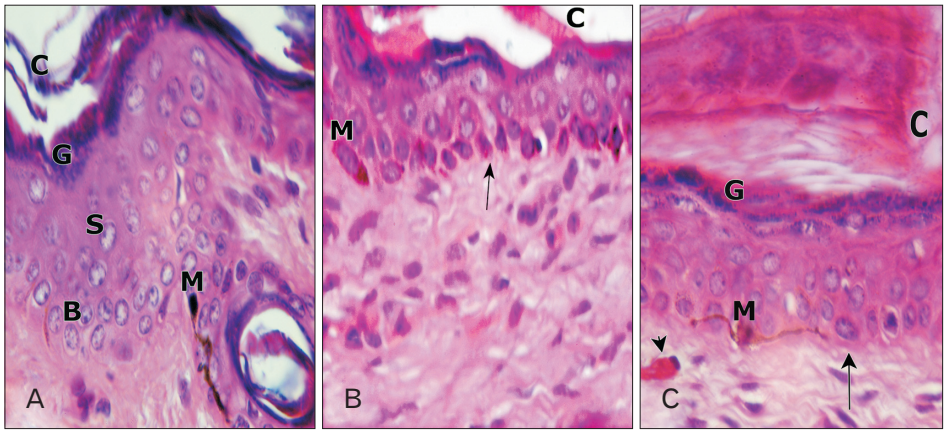

Fig. 1. Photomicrographs of paraffin sections in guinea pig thin skin (H&E, ×400). (A) Group I: epidermal layers; stratum basale (B), stratum spinosum (S), stratum granulosum (G), stratum corneum (C), and melanocyte (M). (B) Group IIA: marked reduction in the epidermal thickness compared to group I, flattened dermoepidermal junction (arrow), swollen corneocyte (C), and melanocyte (M). (C) Group IIB: increased epidermal thickness compared to group IIA, flattened dermo-epidermal junction (arrow), desquamated granule cells in the stratum corneum (C), stratum granulosum (G), melanocyte (M), congested blood capillary (arrowhead).

https://doi.org/10.5115/acb.2017.50.3.187

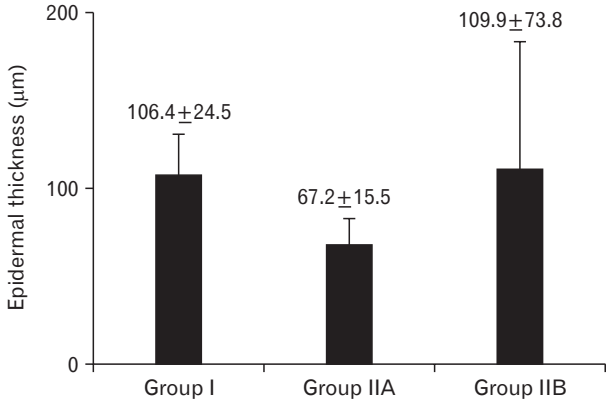

Fig. 2. The mean epidermal thickness (μm) in the studied groups.

Table 2. Mean rete ridges length (μm) in the studied groups

	Group I	Group IIA	Group IIB	*P*-value
Mean±SD	548.4±334.8	223.2±73.8	177.0±71.7	0.001[a]
Range	232.0–1,101.0	104.7–295.3	100.0–284.1	

[a]Group IIA vs. group IIB (*P*>0.05).

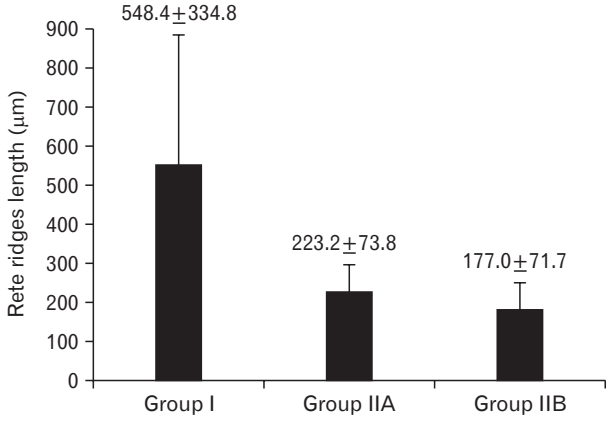

Fig. 3. The mean rete ridges length (μm) in the studied groups.

group IIB was significantly increased compared to group IIA, ranged from 41.3 to 461.2 μm (mean, 109.9±73.8 μm) (Table 1, Fig. 2), accompanied by an increase in the number of granule cells (Fig. 1C). The rete ridges length in group IIA ranged from 104.7 to 295.3 μm (mean, 223.2±73.8 μm) (Table 2, Fig. 3). The rete ridges length in group IIB ranged from 100.0 to 284.1 μm (mean, 177.0±71.7 μm) (Table 2, Fig. 3). Numerous melanocytes with increased melanin pigment were observed in the basal layer of group IIA (Fig. 1B). Their number ranged from 7 to 13 per mm^2 (mean, 10.1±2.0) (Table 3, Fig. 4). But, group IIB revealed occasional melanocytes in the basal layer with few melanin pigments (Fig. 1C). Their number ranged from 1 to 2 per mm^2 (mean, 1.4±0.5) (Table 3, Fig. 4). The

Table 3. Mean number of melanocytes in the studied groups

	Group I	Group IIA	Group IIB	*P*-value
Mean±SD	4.5±1.2	10.1±2.0	1.4±0.5	0.001
Range	3–6	7–13	1–2	

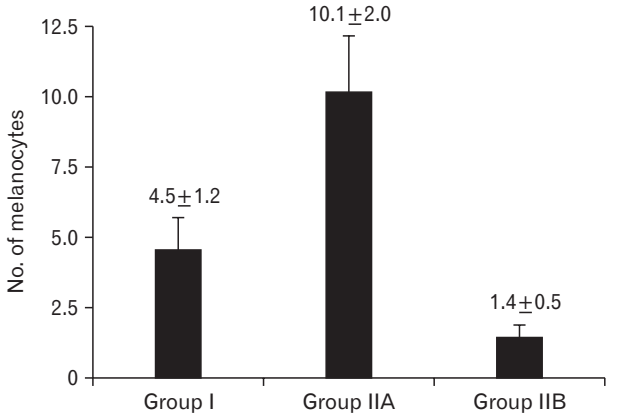

Fig. 4. The mean number of melanocytes in the studied groups.

stratum corneum in group IIA appeared as loosely attached swollen corneocytes (Fig. 1B). Desquamated granular cells were observed in the corneal layer of group IIB (Fig. 1C).

Dermis

Connective tissue fibers

Elastic fibers: Group I revealed thin thread-like elastic fibers which were more numerous around the hair follicles in the reticular dermis (Fig. 5A). But, nicotine treated groups revealed thicker and fewer elastic fibers compared to group I (Fig. 5B, C). Group IIB revealed more reduction in the amount of elastic fibers compared to group IIA.

Collagen fibers: Group I revealed compact bundles of collagen fibers which were thin and parallel to the skin surface in the papillary dermis and thick running in different directions in the reticular dermis (Fig. 6A). But, nicotine treated groups revealed less compactly arranged collagen bundles with spaces between them (Fig. 6B, C). Group IIB revealed more widely separated collagen bundles compared to group IIA (Fig. 6C).

Sebaceous glands

In group I, sebaceous glands were consisted of basal flattened cells and large polyhedral cells that had rounded nuclei and vacuolated cytoplasm (Fig. 7A). Sebaceous glands cells with dark irregular shaped nuclei and accumulated secretion were observed in group IIA (Fig. 7B). But, group IIB revealed sebaceous glands with swollen polyhedral cells containing ac-

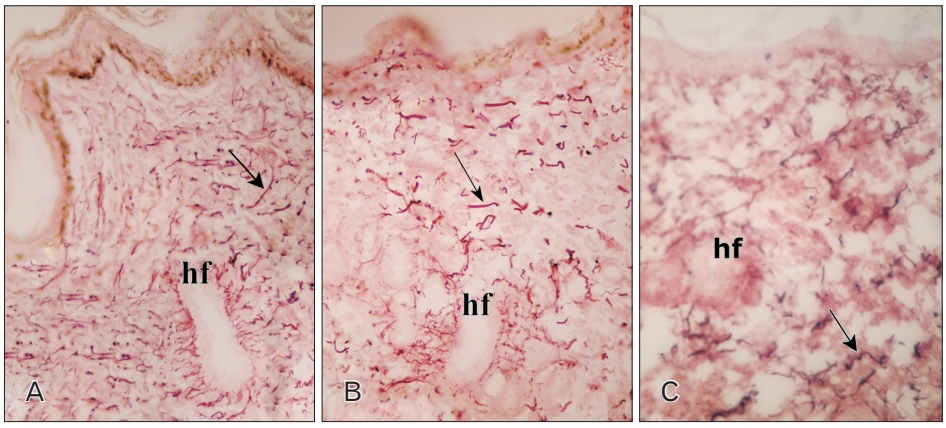

Fig. 5. Photomicrographs of paraffin sections in guinea pig thin skin (Orcein stain, ×400). (A) Group I: thin thread-like elastic fibers (arrow) in the dermis. hf, hair follicle. (B) Group IIA: thicker and fewer elastic fibers (arrow) in the dermis compared to group I. (C) Group IIB: more reduction in the amount of elastic fibers (arrow) in the dermis.

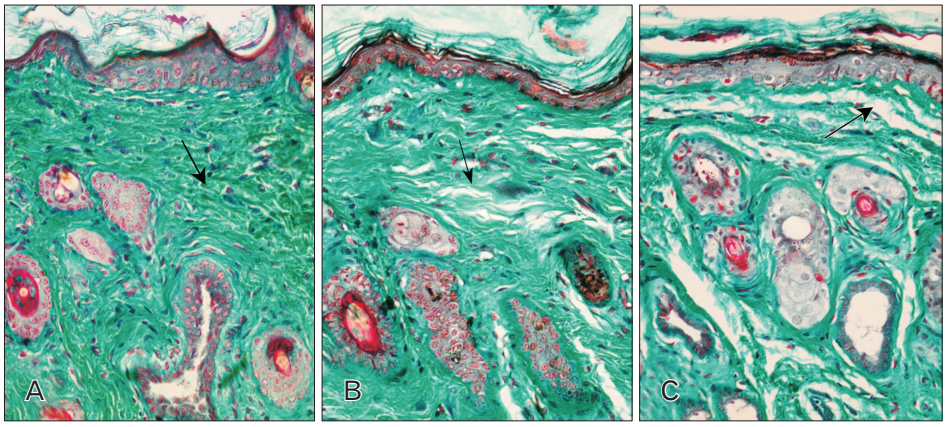

Fig. 6. Photomicrographs of paraffin sections in guinea pig thin skin (Masson's trichrome stain, ×400). (A) Group I: compact bundles of collagen fibers (arrow) in the dermis. (B) Group IIA: less compactly arranged collagen fibers (arrow) in the dermis compared to group I. (C) Group IIB: widely separated collagen fibers (arrow) in the dermis.

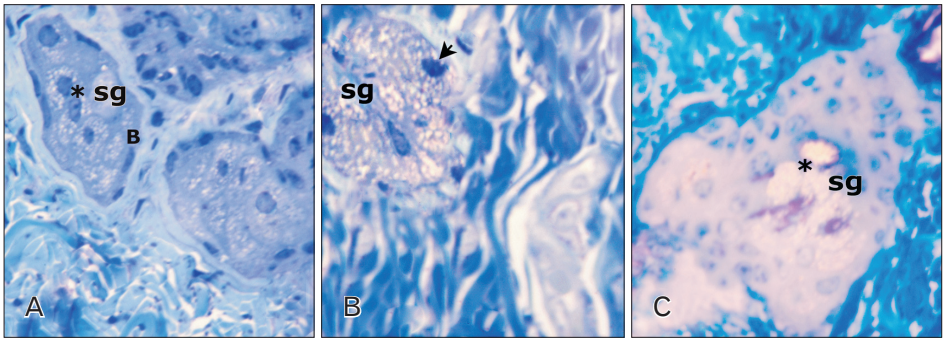

Fig. 7. Photomicrographs of semithin sections in the dermis (Toluidine blue, ×1,000). (A) Group I. sg, sebaceous gland; B, basal flattened cell. Asterisk indicates polyhedral cells with rounded nuclei and vacuolated cytoplasm. (B) Group IIA. Note the dark irregular nucleus (arrowhead). (C) Group IIB. Note the swollen polyhedral cells (asterisk) with accumulated secretion.

cumulated secretion (Fig. 7C).

Mast cells

Group I mast cells, observed in the reticular dermis, contained numerous intracytoplasmic metachromatic granules (Fig. 8A). A reduction in the mast cells granules was observed in nicotine treated groups (Fig. 8B, C).

Electron microscopy

Basal cells

In group I, basal cells were rested on basement membrane where the tonofilaments were condensed to form hemidesmosomes and their lateral plasma membrane extended numerous microfolds. Desmosomes were noticed at the lateral and apical aspects of the cells. Their nuclei were euchromatic with peripheral heterochromatin and the nuclear envelope

https://doi.org/10.5115/acb.2017.50.3.187

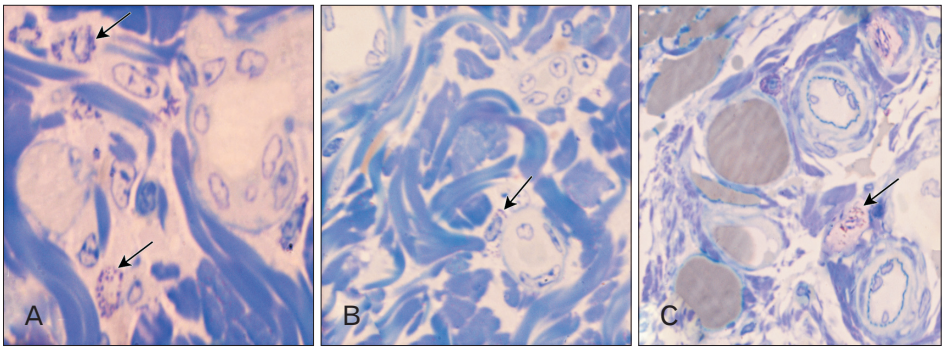

Fig. 8. Photomicrographs of semithin sections in the dermis (Toluidine blue, ×1,000). (A) Group I: mast cells with numerous intracytoplasmic metachromatic granules (arrows). Group IIA (B) and IIB (C): mast cell with few intracytoplasmic metachromatic granules (arrows).

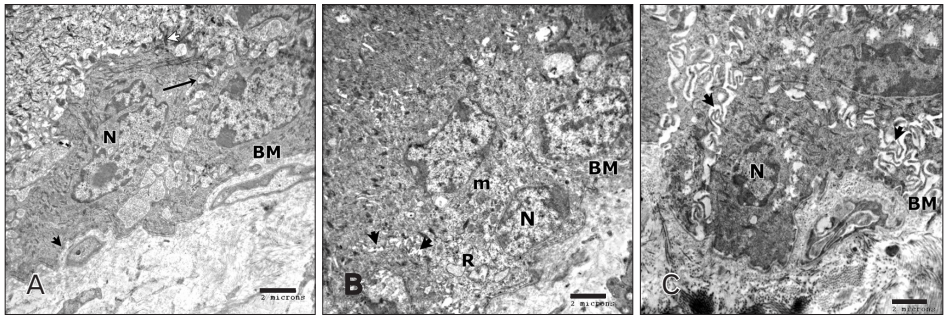

Fig. 9. Electron micrographs, stratum basale (×4,800). (A) Group I: basal cell nucleus (N) with invaginated nuclear envelope. Desmosomes (white arrowhead), membrane microfols (arrow), basement membrane (BM), hemidesmosomes (black arrowhead). (B) Group IIA: basal cell nucleus (N), mitochondria (m), dilated rough endoplasmic reticulum cisternae (R), disrupted desmosomes (arrowheads), basement membrane (BM). (C) Group IIB: basement membrane (BM), basal cell nucleus (N). Note the increased intercellular spaces with prominent lateral plasma membrane microfolds (arrowheads).

was invaginated for a variable distance. Their cytoplasm was electron dense contained numerous free ribosomes, mitochomdria and tonofilaments (Fig. 9A). While, in nicotine treated groups, basal keratinocytes revealed increased intercellular spaces with prominent lateral plasma membrane microfolds, and ill-defined desmosomes at their lateral and apical aspects. They had oval nuclei contained dense clumps of heterochromatin. Their cytoplasm contained numerous mitochondria and dilated rough endoplasmic reticulum (RER) cisternae (Fig. 9B, C).

Melanocytes

In group I, melanocytes cell bodies were observed in the stratum basale. They had rounded nucleus with indented nuclear envelop contained dense clumps of heterochromatin both beneath the nuclear envelope and throughout the nucleoplasm. Their cytoplasm was electron dense contained free ribosomes, mitochondria, tonofilaments, and numerous melanosomes of variable electron densities and shapes; some melanosomes were oval in shape and others were elongated. Desmosomes were found between melanocytes and adjacent keratinocytes. Melanocytes had branching processes containing melanosomes that extended between neighboring keratinocytes of the basal and lower spinous cell layers (Fig. 10A). Group IIA melanocytes were less electron dense compared to group I. Melanosomes were mainly found in the periphery of the cell body and the extending processes. Disruption of desmosomal junctions was observed between melanocytes and adjacent keratinocytes (Fig. 10B). But, in group IIB melanocytes couldn't be distinguished.

Merkel cells

In group I, Merkel cells were observed in the stratum basale resting on the basal lamina and related to peripheral nerve terminals. They had rounded nucleus with indented nuclear envelop contained dense clumps of heterochromatin. Their cytoplasm characterized by small dense cored rounded basal granules. Few RER, mitochondria and free ribosomes were also observed (Fig. 11A). Group IIA Merkel cells revealed convoluted hyperchromatic nucleus with depleted granules (Fig. 11B). But, in group IIB Merkel cells couldn't be distinguished.

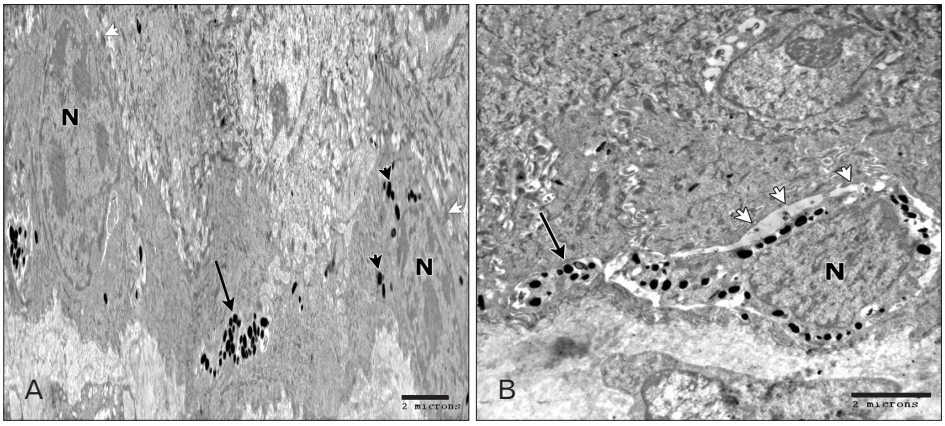

Fig. 10. Electron micrographs, melanocytes (×4,800). (A) Group I: intracytoplasmic melanosomes (black arrowheads), nucleus (N). Note the branching process (arrow) containing melanosomes. White arrowhead indicates desmosomes. (B) Group IIA: disrupted desmosomes (white arrowheads) between melanocyte and adjacent keratinocyte, nucleus (N). Note the peripheral melanosomes and the process (arrow) containing melanosomes.

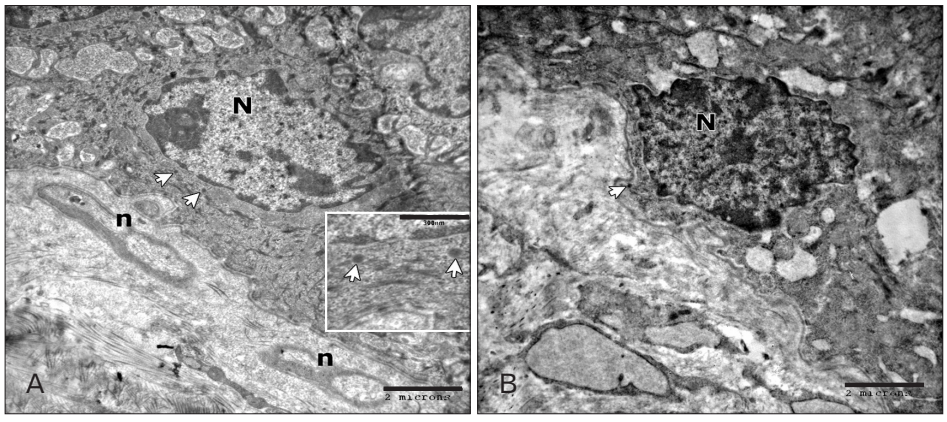

Fig. 11. Electron micrographs, Merkel cells (×7,200). (A) Group I: small dense cored rounded basal granules (arrowheads), nucleus (N). Note, the peripheral nerve terminals (n). Inset: The dense cored granules (arrowheads) at higher magnification (×15,000). (B) Group IIA: convoluted hyperchromatic nucleus (N), small dense cored rounded basal granule (arrowhead).

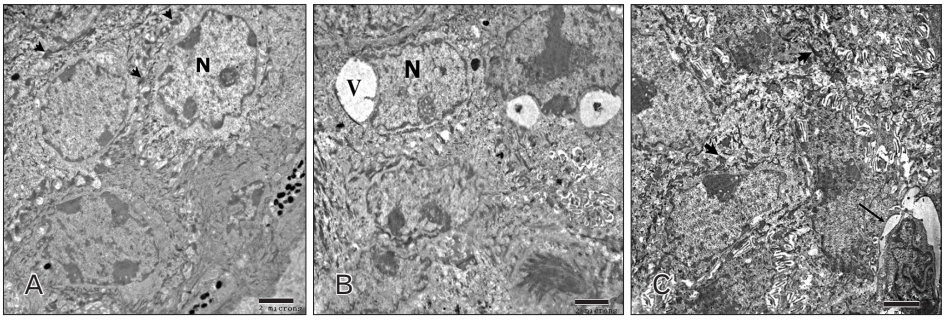

Fig. 12. Electron micrographs, stratum spinosum. (×4,800). (A) Group I: nucleus (N) with prominent nucleoli. Tonofilaments are obvious at the sites of desmosomes (arrowheads). (B) Group IIA: cytoplasmic vacuoles (V), nucleus (N). (C) Group IIB: disrupted desmosomes (arrow), tonofilaments (arrowheads).

Stratum spinosum

In group I, keratinocytes in the stratum spinosum had rounded to oval nuclei. Their nuclei were euchromatic with few peripheral heterochromatin and revealed prominent nucleoli and the nuclear envelope was invaginated for a variable distance. Their cytoplasm contained tonofilaments that were condensed at the sites of desmosomes (Fig. 12A). In group IIA, keratinocytes in the stratum spinosum had irregularly shaped nuclei with peripheral clumped chromatin and some of them contained prominent nucleolus. Their cytoplasm contained vacuoles of variable sizes and some of them were located near the nuclei causing their indentation. Irregular tonofilaments distribution with increased intercellular spaces were observed (Fig. 12B). Some melanosomes were observed among tonofilaments of keratinocytes. Occasional apoptotic cells with margination of condensed chromatin were also observed (Fig. 13B). In group IIB, keratinocytes in the stratum spinosum revealed conspicuous irregular tonofilaments distribution with increased inter-cellular spaces and disruption of desmosomes (Fig. 12C).

https://doi.org/10.5115/acb.2017.50.3.187

Langerhans cells

In group I, occasional Langerhans cells were observed among the spinous cells. They had folded or lobulated nucleus with peripheral dense clumps of heterochromatin. Their cytoplasm contained the characteristic rod shaped granules with bulbous expansion. These granules were mainly found in the periphery of the cells. They had no filaments, and no desmosomes could be seen along their cell membrane (Fig. 14A). In group IIA, Langerhans cells exhibited convoluted nucleus with few peripheral heterochromatin and their cytoplasm contained few rod shaped granules (Fig. 14B). But, in group IIB Langerhans cells couldn't be distinguished.

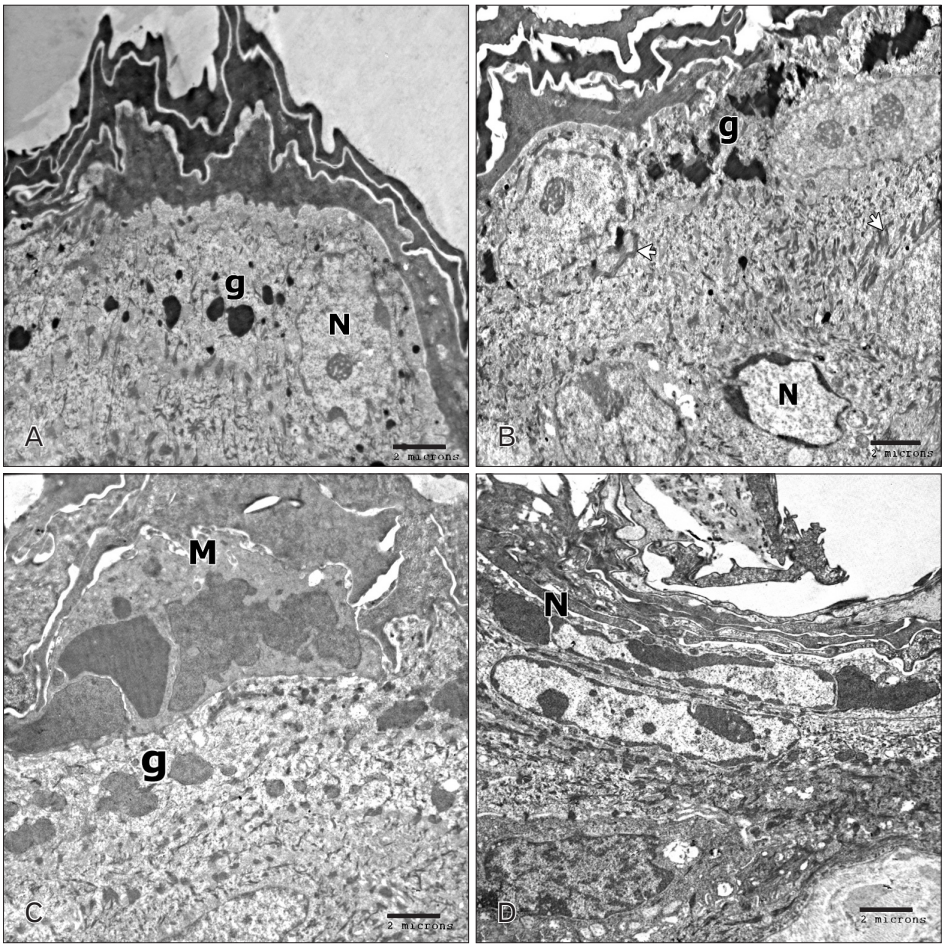

Fig. 13. Electron micrographs, stratum granulosum (×4,800). (A) Group I: keratohyaline granules (g), nucleus (N). (B) Group IIA: large clumps of keratohyaline granules (g), thick bundles of tonofilaments (white arrowhead). Note the apoptotic nucleus (N) with peripheral marginated chromatin. (C) Group IIB: a cell at prophase stage of mitosis (M). (D) Group IIB: apoptotic fragmented nucleus (N).

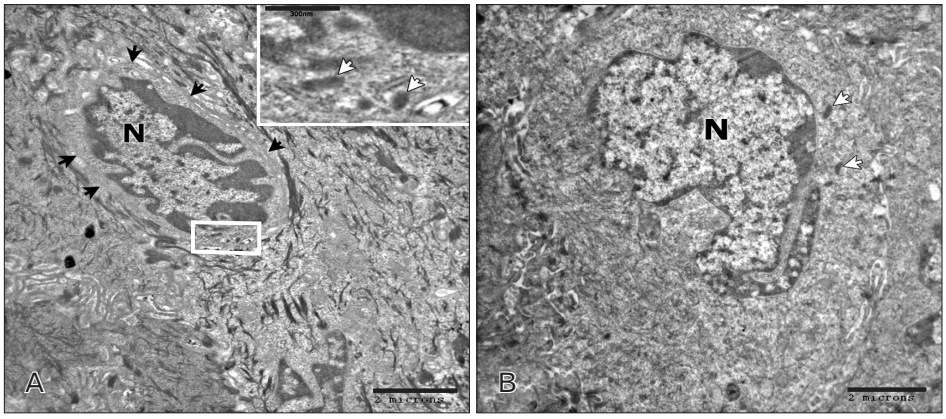

Fig. 14. Electron micrographs, Langerhans cells (×7,200). (A) Group I: folded nucleus (N), rod shaped granules with bulbous expansion (white rectangle). No filaments or desmosomes along its cell membrane (black arrowheads). Inset: the rod shaped granules (white arrowheads) at higher magnification (×15,000). (B) Group IIA: convoluted nucleus (N), rod shaped granules (white arrowheads).

Stratum granulosum

In group I, keratinocytes in the stratum granulosum showed oval euchromatic nuclei with prominent nucleoli and their cytoplasm contained variable sized keratohyaline granules and tonofilaments (Fig. 13A). In nicotine treated groups group, large clumps of keratohyaline granules and thick bundles of tonofilaments were observed in the stratum granulosum (Fig. 13B, C). Moreover, some keratinocytes in the stratum granulosum of group IIB revealed apoptotic nuclei with margination of condensed chromatin (Fig. 13D). Others were in prophase stage of mitosis; the nuclear enveloped disappeared and the chromosomes appeared condensed (Fig. 13C).

Sebaceous glands

In group I, sebaceous glands were consisted of two types of cells; flattened basal cells and polyhedral cells. The former had euchromatic oval nuclei with few peripheral heterochromatin. Their cytoplasm contained mainly free ribosomes. Some basal cells were in mitosis; chromosomes had almost completed their alignment on the metaphase plate. While, polyhedral cells had rounded to oval nuclei and their cytoplasm was filled with lipid droplets; most of them were bleached away giving it a "honey combed" appearance (Fig. 15A). In nicotine treated groups, cells of the sebaceous glands exhibited apoptotic nuclei at various stages; margination of condensed chromatin and fragmentation with partially retained intracytoplasmic secretion (Fig. 15B, C).

Mast cells

In group I, mast cells were characteristically observed near the blood capillaries and nerve fibers in the dermis. They had indented nuclei contained peripheral heterochromatin clumps. Their cytoplasm contained numerous electron dense granules (Fig. 16A). In nicotine treated groups, mast cells contained few intracytoplasmic secretory granules and dilated RER cisternae (Fig. 16B, C).

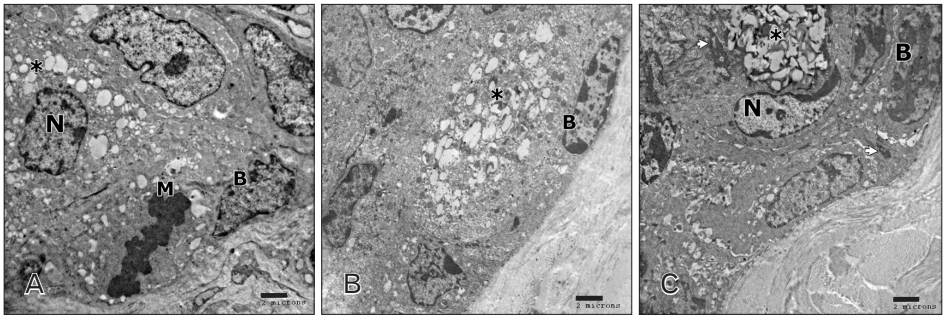

Fig. 15. Electron micrographs, dermis, sebaceous gland (×3,600). (A) Group I: a flattened basal cell (B), basal cell in mitosis (M), nucleus of polyhedral cell (N), intracytoplasmic lipid droplets (asterisk). (B) Group IIA: basal cell (B) with apoptotic nucleus. Retained intracytoplasmic secretion (asterisk). (C) Group IIB: basal cell (B), apoptotic nucleus (N) with peripheral marginated chromatin, apoptotic fragmented nuclei (arrowheads), retained intracytoplasmic secretion (asterisk).

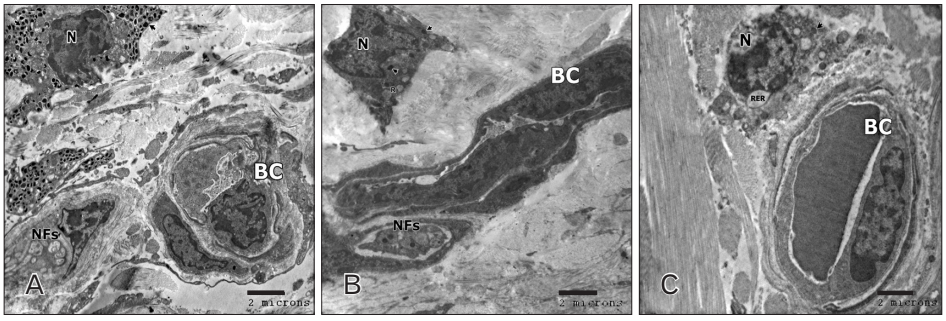

Fig. 16. Electron micrographs, dermis, mast cell (×3,600). (A) Group I: numerous intra-cytoplasmic granules (arrowhead). Nucleus (N). Note the blood capillary (BC) and the nerve fibers (NFs). (B) Group IIA: few intra-cytoplasmic granules (arrowhead), dilated rough endoplasmic reticulum (RER) cisternae (R), nucleus (N). Note the blood capillary (BC) and the nerve fibers (NFs). (C) Group IIB: dilated RER, nucleus (N). Note the few intra-cytoplasmic granules (arrowhead). Congested blood capillary (BC).

https://doi.org/10.5115/acb.2017.50.3.187

Discussion

Guinea pig skin serves as a good model for human skin studies [16, 17]. In this study, the back thin skin in nicotine treated guinea pigs revealed flattening of the DEJ and reduced rete ridges formation. This finding was more pronounced in high dose nicotine treated group. A comparable study between unexposed (upper inner arm) and exposed (dorsal forearm) sites of elderly people was done by Lavker [18]. Senile skin revealed a relatively flat dermal-epidermal junction devoid of the micro projections of basal cells into the dermis, in both sites [18]. Similarly, Baumann [19] observed reduced rete ridges formation in abdominal skin of aged man (61–80 years old). This might lead to increased fragility of the skin and reduced nutrient transfer between the dermal and epidermal layers [19].

Statistical results of this study revealed a significant reduction ($P<0.05$) in the mean thickness of the epidermis in low dose nicotine treated group. The apoptotic keratinocytes observed ultrastructurally in the stratum spinosum might correlate to the decreased epidermal thickness. Similarly, Branchet et al. [20] observed a thinner epidermis in aged men skin. Also, Oriá et al. [21] observed a significant decrease in the epidermal thickness of patients aged >60 years. Oxidative stress and accumulation of free radicals in keratinocytes accompanying aging and tobacco smoking might influence the genetic program and caused cell death [22, 23]. Ozguner et al. [22] demonstrated a significant decrease in plasma levels of melatonin (a powerful endogenous antioxidant) in cigarette smokers. In addition, it was reported that nicotine activates the nuclear transcription factor κB, which is involved in cell death [24]. Moreover, the epidermal thinning and the flattening of the DEJ might cause cutaneous atrophy [25]. In contrast, high dose nicotine treated group revealed an increase in the mean epidermal thickness. This finding could correlate to the increased number of granule cells accompanied with mitosis which observed in keratinocytes of the stratum granulosum ultrastructurally in high dose nicotine treated group. Several studies have confirmed that smokers tend to have an extensive and severe psoriasis (scaly patches of skin) [26-28].

In addition, this study revealed changes in the stratum corneum in nicotine treated groups. It appeared as loosely attached swollen corneocytes in low dose nicotine treated group. But, high dose treated group exhibited desquamated granular cells in the corneal layer. These findings might reflect a decelerated cell turnover and account for the formation of heaps of corneocytes that render the skin surface rough and dull in appearance [29].

Numerous melanocytes with increased melanin pigment were observed in this study in low dose nicotine treated group. Ultrastructurally, melanosomes were mainly found in the periphery of the melanocytes cell body and their extending processes. Moreover, melanosomes were observed among tonofilaments of keratinocytes. In agreement, it was reported that in tobacco-users the melanocytes are stimulated to produce melanin granules and to distribute them out to the surrounding keratinocyres. It was reported that smokers can typically be identified by characteristic cutaneous and mucosal discoloration [30, 31]. Nicotine, which can act as a precursor in melanin synthesis, is capable of irreversibly binding melanin and accumulating in melanin-containing tissues [32]. Tadakamadla et al. [33] concluded that nicotine and benzopyrene in the tobacco smoke stimulated the production of melanin from the melanocytes. Also, Nakamura et al. [34] provided the evidence that tobacco smoke enhances pigmentation in vitro. They also suggested that the increase in pigmentation might involve β-catenin– and aryl hydrocarbon receptors–mediated mechanisms inside human melanocytes.

Keratinocytes in nicotine treated groups in this study revealed increased inter-cellular spaces with disrupted desmosomes. This finding was more pronounced in high dose nicotine treated group. Desmosomes are intercellular junctions that provide strong adhesion between cells. Because they also link intracellularly to the intermediate filament cytoskeleton, they form the adhesive bonds in a network that gives mechanical strength to tissues. The desmosome-intermediate filament complex is a network or scaffolding that maintains the integrity of such tissues. When desmosomal adhesion fails, tissues that are subjected to mechanical stress may fall apart [35]. Also, Xin et al. [36] reported defective epidermal permeability barrier in heavy cigarette smokers.

In this study, dermal elastic fibers became thickened and fewer in nicotine treated groups. Consistently, Wulf et al. [37] reported thickened, tangled, and degraded elastic fibers in skin areas exposed to solar radiation. In agreement, Ortolan et al. [38] observed degenerated, thickened, tangled, and often fragmented elastic fibers in preauricular skin of elderly individuals (70 years). Also, Bosset et al. [39] found that the network of elastic fiber in superficial papillary dermis were diminished or absent in sun exposed facial skin of Caucasian man but present in sun protected area. But, Ortonne and Marks [40] observed large quantities of abnormal thickened

elastic fibers "elastosis" in photo aged human. According to Ortonne and Marks [40], the thickened elastic fibers "elastosis" resemble elastin biochemically, although it is disorganized and the proportion of several of its constituents is abnormal [37]. Elastosis might reveal abnormal synthetic activity of fibroblasts via cytokine released from epidermal keratinocytes [41]. As elastic fibers are responsible for the physiological elasticity and resilience of the skin, the degeneration of these fibers promotes the reduction of skin elasticity and wrinkle formation [42].

Moreover, this study revealed disorganized dermal collagen bundles with spaces between them in nicotine treated groups. Similarly, Ortolan et al. [38] reported disorganization and fragmentation of collaged fibers in aged skin. This finding could attribute to the oxidative stress caused by nicotine. It was reported that the oxidative stress induced by tobacco smoking caused insufficient oxygen supply to the skin resulting in tissue ischaemia and blood vessel occlusion inducing matrix metalloproteinase 1, an enzyme that specifically degrades collagen. Moreover, fibroblasts were vulnerable to the accumulation of oxidized proteins following oxidative stress [43]. Collagen fibers in the dermis provide tensile strength to the skin [44] and its disorganization and fragmentation have been reported as the cause of wrinkle development [25].

This study revealed accumulated intracytoplasmic lipid secretion in sebaceous glands of nicotine treated groups. In addition, various stages of apoptosis were observed in sebaceous gland cells especially with high dose nicotine. It was reported that tobacco smoking stimulates the production of androgen (male hormone), that signals the production of sebum in the sebaceous glands. As these glands produce more oil, pores are more easily clogged, resulting in inflammatory, often painful acne lesions [45, 46].

Mast cells in the reticular dermis of nicotine treated groups in this study exhibited fewer intra-cytoplasmic granules. In agreement, Kindt et al. [47] and Mishra et al. [48] documented that nicotine suppresses mast cell function in human skin through the nicotinic acetylcholine receptors. Mishra et al. [48] suggested that nicotine affects the late degranulation phase of mast cell activation. Nicotine also affected the mast cell function in the lung [49]. It suppresses the allergen induced production of cysteinyl leukotrienes (LTC4) and inflammatory cytokines in animal models of allergic asthma [49].

In conclusion, nicotine induced structural changes of adult male guinea pig thin skin. These changes were more pronounced with high dose nicotine administration.

Acknowledgements

Assiut University is the source of funding for this research.

References

1. Siegmund B, Leitner E, Pfannhauser W. Determination of the nicotine content of various edible nightshades (Solanaceae) and their products and estimation of the associated dietary nicotine intake. J Agric Food Chem 1999;47:3113-20.
2. Mayer B. How much nicotine kills a human? Tracing back the generally accepted lethal dose to dubious self-experiments in the nineteenth century. Arch Toxicol 2014;88:5-7.
3. Caponnetto P, Campagna D, Papale G, Russo C, Polosa R. The emerging phenomenon of electronic cigarettes. Expert Rev Respir Med 2012;6:63-74.
4. Misery L. Nicotine effects on skin: are they positive or negative? Exp Dermatol 2004;13:665-70.
5. Tortora GJ, Grabowski SR. Principles of anatomy and physiology. New York: Harper Collins College Publishers; 1993.
6. Kadunce DP, Burr R, Gress R, Kanner R, Lyon JL, Zone JJ. Cigarette smoking: risk factor for premature facial wrinkling. Ann Intern Med 1991;114:840-4.
7. Yin L, Morita A, Tsuji T. Skin aging induced by ultraviolet exposure and tobacco smoking: evidence from epidemiological and molecular studies. Photodermatol Photoimmunol Photomed 2001;17:178-83.
8. Koh JS, Kang H, Choi SW, Kim HO. Cigarette smoking associated with premature facial wrinkling: image analysis of facial skin replicas. Int J Dermatol 2002;41:21-7.
9. Fore J. A review of skin and the effects of aging on skin structure and function. Ostomy Wound Manage 2006;52:24-35.
10. Farage MA, Miller KW, Elsner P, Maibach HI. Intrinsic and extrinsic factors in skin ageing: a review. Int J Cosmet Sci 2008;30:87-95.
11. Matta SG, Balfour DJ, Benowitz NL, Boyd RT, Buccafusco JJ, Caggiula AR, Craig CR, Collins AC, Damaj MI, Donny EC, Gardiner PS, Grady SR, Heberlein U, Leonard SS, Levin ED, Lukas RJ, Markou A, Marks MJ, McCallum SE, Parameswaran N, Perkins KA, Picciotto MR, Quik M, Rose JE, Rothenfluh A, Schafer WR, Stolerman IP, Tyndale RF, Wehner JM, Zirger JM. Guidelines on nicotine dose selection for *in vivo* research. Psychopharmacology (Berl) 2007;190:269-319.
12. Abdel-Hafez AM, Elgayar SA, Husain OA, Thabet HS. Effect of nicotine on the structure of cochlea of guinea pigs. Anat Cell Biol 2014;47:162-70.
13. Drury RA, Wallington EA. Carelton's histology technique. 5th ed. Oxford: Oxford University Press; 1980.
14. Gupta PD. Ultrastructural study on semithin section. Sci Tools 1983;30:6-7.

https://doi.org/10.5115/acb.2017.50.3.187

15. Inan S, Oztukcan S, Vatansever S, Ermertcan AT, Zeybek D, Oksal A, Giray G, Muftuoglu S. Histopathological and ultrastructural effects of glycolic acid on rat skin. Acta Histochem 2006;108:37-47.
16. Barbero AM, Frasch HF. Pig and guinea pig skin as surrogates for human in vitro penetration studies: a quantitative review. Toxicol In Vitro 2009;23:1-13.
17. Frasch HF, Barbero AM. A paired comparison between human skin and hairless guinea pig skin *in vitro* permeability and lag time measurements for 6 industrial chemicals. Cutan Ocul Toxicol 2009;28:107-13.
18. Lavker RM. Structural alterations in exposed and unexposed aged skin. J Invest Dermatol 1979;73:59-66.
19. Baumann L. Skin ageing and its treatment. J Pathol 2007;211:241-51.
20. Branchet MC, Boisnic S, Frances C, Robert AM. Skin thickness changes in normal aging skin. Gerontology 1990;36:28-35.
21. Oriá RB, Ferreira FV, Santana EN, Fernandes MR, Brito GA. Study of age-related changes in human skin using histomorphometric and autofluorescence approaches. An Bras Dermatol 2003;78:425-34.
22. Ozguner F, Koyu A, Cesur G. Active smoking causes oxidative stress and decreases blood melatonin levels. Toxicol Ind Health 2005;21:21-6.
23. Deruy E, Gosselin K, Vercamer C, Martien S, Bouali F, Slomianny C, Bertout J, Bernard D, Pourtier A, Abbadie C. MnSOD upregulation induces autophagic programmed cell death in senescent keratinocytes. PLoS One 2010;5:e12712.
24. Barr J, Sharma CS, Sarkar S, Wise K, Dong L, Periyakaruppan A, Ramesh GT. Nicotine induces oxidative stress and activates nuclear transcription factor kappa B in rat mesencephalic cells. Mol Cell Biochem 2007;297:93-9.
25. Fisher GJ, Kang S, Varani J, Bata-Csorgo Z, Wan Y, Datta S, Voorhees JJ. Mechanisms of photoaging and chronological skin aging. Arch Dermatol 2002;138:1462-70.
26. Fortes C, Mastroeni S, Leffondre K, Sampogna F, Melchi F, Mazzotti E, Pasquini P, Abeni D. Relationship between smoking and the clinical severity of psoriasis. Arch Dermatol 2005;141:1580-4.
27. Setty AR, Curhan G, Choi HK. Smoking and the risk of psoriasis in women: Nurses' health study II. Am J Med 2007;120:953-9.
28. Li W, Han J, Qureshi AA. Smoking and risk of incident psoriatic arthritis in US women. Ann Rheum Dis 2012;71:804-8.
29. Soroka Y, Ma'or Z, Leshem Y, Verochovsky L, Neuman R, Brégégère FM, Milner Y. Aged keratinocyte phenotyping: morphology, biochemical markers and effects of Dead Sea minerals. Exp Gerontol 2008;43:947-57.
30. Wallstrom M, Sand L, Nilsson F, Hirsch JM. The long-term effect of nicotine on the oral mucosa. Addiction 1999;94:417-23.
31. Hanioka T, Tanaka K, Ojima M, Yuuki K. Association of melanin pigmentation in the gingiva of children with parents who smoke. Pediatrics 2005;116:e186-90.
32. Claffey DJ, Stout PR, Ruth JA. 3H-nicotine, 3H-flunitrazepam, and 3H-cocaine incorporation into melanin: a model for the examination of drug-melanin interactions. J Anal Toxicol 2001;25:607-11.
33. Tadakamadla J, Kumar S, Nagori A, Tibdewal H, Duraiswamy P, Kulkarni S. Effect of smoking on oral pigmentation and its relationship with periodontal status. Dent Res J (Isfahan) 2012;9:S112-4.
34. Nakamura M, Ueda Y, Hayashi M, Kato H, Furuhashi T, Morita A. Tobacco smoke-induced skin pigmentation is mediated by the aryl hydrocarbon receptor. Exp Dermatol 2013;22:556-8.
35. Garrod D, Chidgey M. Desmosome structure, composition and function. Biochim Biophys Acta 2008;1778:572-87.
36. Xin S, Ye L, Man G, Lv C, Elias PM, Man MQ. Heavy cigarette smokers in a Chinese population display a compromised permeability barrier. Biomed Res Int 2016;2016:9704598.
37. Wulf HC, Sandby-Møller J, Kobayasi T, Gniadecki R. Skin aging and natural photoprotection. Micron 2004;35:185-91.
38. Ortolan MC, Biondo-Simões MD, Valenga Baroni ED, Auersvald A, Auersvald LA, Netto MR, Biondo-Simões R. Influence of aging on the skin quality of white-skinned women: the role of collagen, elastic material density, and vascularization. Rev Bras Cir Plast 2013;28:41-8.
39. Bosset S, Bonnet-Duquennoy M, Barré P, Chalon A, Lazou K, Kurfurst R, Bonté F, Schnébert S, Disant F, Le Varlet B, Nicolas JF. Decreased expression of keratinocyte beta1 integrins in chronically sun-exposed skin *in vivo*. Br J Dermatol 2003;148:770-8.
40. Ortonne JP, Marks R. Photodamaged skin: clinical signs, causes and management. London: Martin Dunitz Ltd.; 1999.
41. Imokawa G, Nakajima H, Ishida K. Biological mechanisms underlying the ultraviolet radiation-induced formation of skin wrinkling and sagging II: over-expression of neprilysin plays an essential role. Int J Mol Sci 2015;16:7776-95.
42. El-Domyati M, Attia S, Saleh F, Brown D, Birk DE, Gasparro F, Ahmad H, Uitto J. Intrinsic aging vs. photoaging: a comparative histopathological, immunohistochemical, and ultrastructural study of skin. Exp Dermatol 2002;11:398-405.
43. Merker K, Sitte N, Grune T. Hydrogen peroxide-mediated protein oxidation in young and old human MRC-5 fibroblasts. Arch Biochem Biophys 2000;375:50-4.
44. Gray H, Williams PL, Bannister LH. Gray's anatomy: the anatomical basis of medicine and surgery. 38th ed. New York: Churchill Livingstone; 1995.
45. Zouboulis CC, Eady A, Philpott M, Goldsmith LA, Orfanos C, Cunliffe WC, Rosenfield R. What is the pathogenesis of acne? Exp Dermatol 2005;14:143-52.
46. Zouboulis CC, Baron JM, Bohm M, Kippenberger S, Kurzen H, Reichrath J, Thielitz A. Frontiers in sebaceous gland biology and pathology. Exp Dermatol 2008;17:542-51.
47. Kindt F, Wiegand S, Niemeier V, Kupfer J, Löser C, Nilles M, Kurzen H, Kummer W, Gieler U, Haberberger RV. Reduced expression of nicotinic alpha subunits 3, 7, 9 and 10 in lesional and nonlesional atopic dermatitis skin but enhanced expression of alpha subunits 3 and 5 in mast cells. Br J Dermatol 2008;159:847-57.

48. Mishra NC, Rir-sima-ah J, Boyd RT, Singh SP, Gundavarapu S, Langley RJ, Razani-Boroujerdi S, Sopori ML. Nicotine inhibits Fc epsilon RI-induced cysteinyl leukotrienes and cytokine production without affecting mast cell degranulation through alpha 7/alpha 9/alpha 10-nicotinic receptors. J Immunol 2010;185:588-96.

49. Mishra NC, Rir-Sima-Ah J, Langley RJ, Singh SP, Peña-Philippides JC, Koga T, Razani-Boroujerdi S, Hutt J, Campen M, Kim KC, Tesfaigzi Y, Sopori ML. Nicotine primarily suppresses lung Th2 but not goblet cell and muscle cell responses to allergens. J Immunol 2008;180:7655-63.